Equation of State of Neutron Star Matter

J. M. Lattimer

Department of Physics & Astronomy

lectromagnetic Signatures of R-Process Nucleosynthesis in Neutron Star Merge
INT, Seattle, Washington
24 July - 18 August, 2017

Outline

- The Unitary Gas Constraint on the Nuclear Symmetry Energy
- Constraints from Nuclear Physics and the Maximum Mass on Neutron Star Universal Structure
- How the Possibility of Hybrid Stars Loosens Constraints
- Observational Estimates of Neutron Star Radii and Their Problems

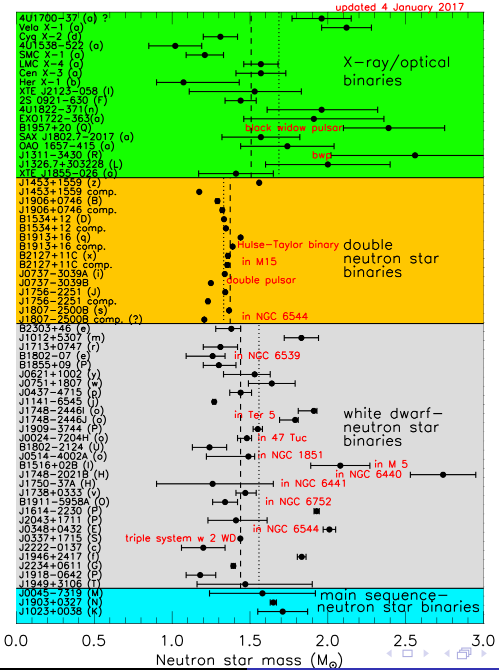

vanKerkwijk 2010

Romani et al. 2012

Although simple average mass of w.d. companions is 0.23 $M_\odot$ larger, weighted average is 0.07 $M_\odot$ larger

Demorest et al. 2010

Fonseca et al. 2016

Antoniadis et al. 2013

Barr et al. 2016

Causality + GR Limits and the Maximum Mass

A lower limit to the maximum mass sets a lower limit to the radius for a given mass.

Similarly, a precision upper limit to R, with a well-measured mass, sets an upper limit to the maximum mass.

$R_{1.4} > 8.15$ km if $M_{max} \geq 2.01 M_\odot$.

$M - R$ curves for minimally compact EOS

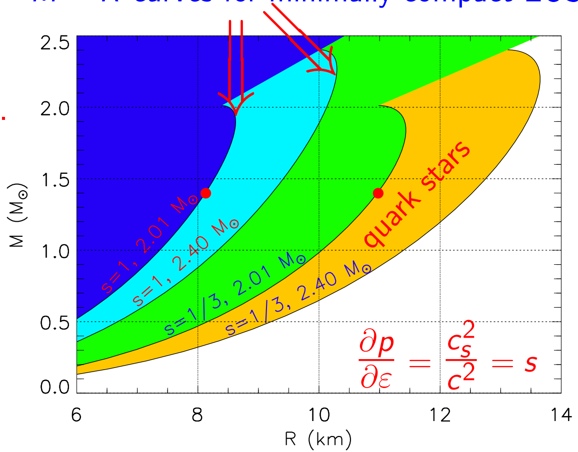

If quark matter exists in the interior, the minimum radii are substantially larger.

The Unitary Gas

The **unitary gas** is an idealized system consisting of fermions interacting via a pairwise zero-range s-wave interaction with an infinite scattering length:

As long as the scattering length $a >> k_F^{-1}$ (interparticle spacing), and the range of the interaction $R << k_F^{-1}$, the properties of the gas are universal in the sense they don't depend on the details of the interaction.

The sole remaining length scale is $k_F = (3\pi^2 n)^{1/3}$, so the unitary gas energy is a constant times the Fermi energy $\hbar^2 k_F^2/(2m)$:

$$E_{\rm UG} = \xi_0 \frac{3\hbar^2 k_F^2}{10m}.$$

$\xi_0 \simeq 0.37$ is known as the **Bertsch** parameter, measured in cold-atom experiments.

The Unitary Gas as Analogue of the Neutron Gas

A pure neutron matter (PNM) gas differs from the unitary gas:

- $|a| \simeq 18.5$ fm; $|ak_F|^{-1} \simeq 0.03$ for $n = n_s$.
- $R \simeq 2.7$ fm; $Rk_F \approx 4.5$ for $n = n_s$.
- Repulsive 3-body interactions are additionally necessary for neutron matter to fit the energies of light nuclei.
- Neutron matter has potentially atractive p-wave and higher-order interactions.

The first three imply $E_{\rm PNM} > E_{\rm UG}$:

- $\xi \simeq \xi_0 + 0.6|ak_F|^{-1} + \dots \qquad |ak_F|^{-1} << 1$
- $\xi \simeq \xi_0 + 0.12Rk_F + \dots \qquad Rk_F << 1$

A reasonable conjecture would appear to be ($u = n/n_s$)

$$E_{\rm PNM}(u) = E(u, Y_p = 0) \geq E_{\rm UG,0}u^{2/3} \simeq 12.6u^{2/3}\ {\rm MeV}$$

Comparison to Neutron Matter Calculations

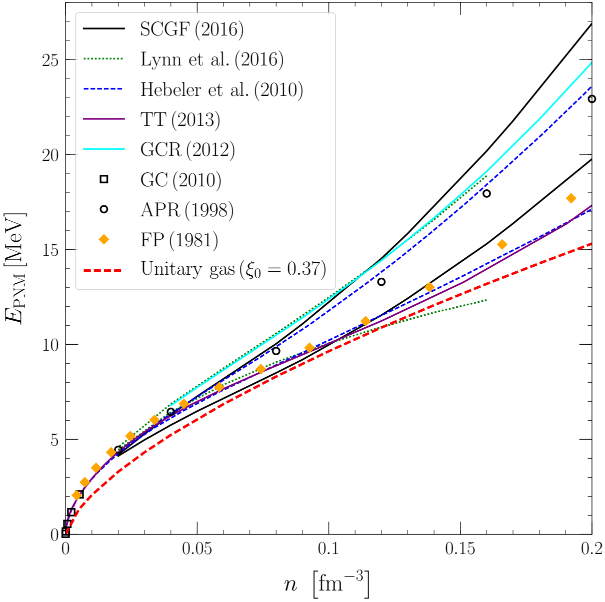

Consequences for the Nuclear Symmetry Energy

$$S(u) = E_{\rm PNM} - E(u, Y_p = 1/2).$$

A good approximation for the Y_p−dependence of E is

$$S(u) \simeq \frac{1}{8}\frac{\partial^2 E(u, Y_p)}{\partial Y_p^2}.$$

Near n_s,

$$S(u) \simeq S_0 + \frac{L}{3}(u-1) + \frac{K_{sym}}{18}(u-1)^2 + \cdots$$

$$E(u, Y_p = 1/2) \simeq -B + \frac{K_s}{18}(u-1)^2 + \cdots$$

In this case, the unitary gas conjecture is

$$S(u) > E_{\rm UG,0}u^{2/3} - \left[-B + \frac{K_s}{18}(u-1)^2 + \cdots\right] \equiv S^{\rm LB}(u)$$

Thus, the symmetry energy parameters S_0 and L must satisfy

$$S(u=1) = S_0 \geq S_0^{\rm LB} = E_{\rm UG,0} + B \simeq 28.5 \text{ MeV}$$

$$L(u=1) = L_0 = 3\left(udS/du\right)_{u=1} = 2E_{\rm UG,0} \simeq 25.2\text{MeV}$$

$$S_0 > S_0^{\rm LB}: \quad \left(S = S^{\rm LB}\right)_{u_t}, \left(dS/du = dS^{\rm LB}/du\right)_{u_t}$$

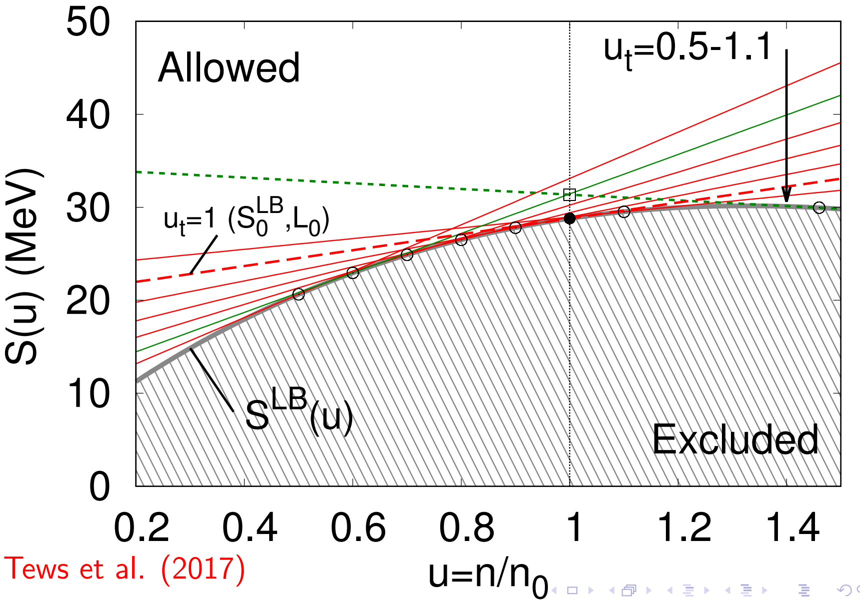

Tews et al. (2017)

Symmetry Parameter Exclusions

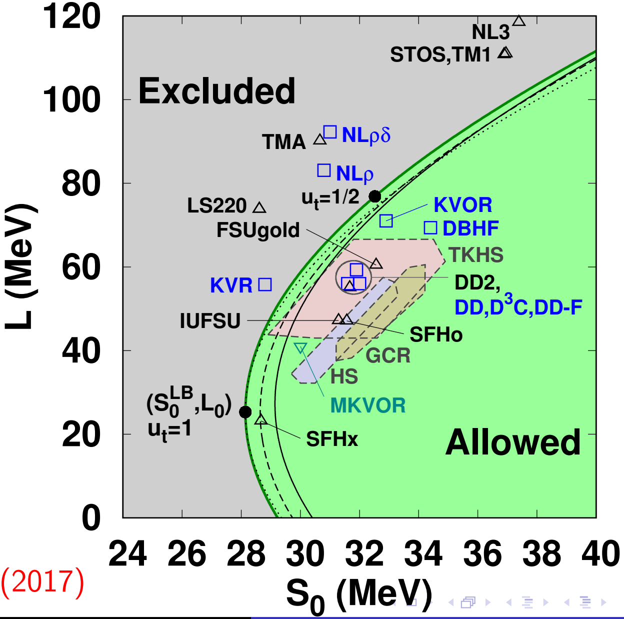

Tews et al. (2017)

Symmetry Parameter Correlations

Compilations from Dutra et al. (2012, 2014)

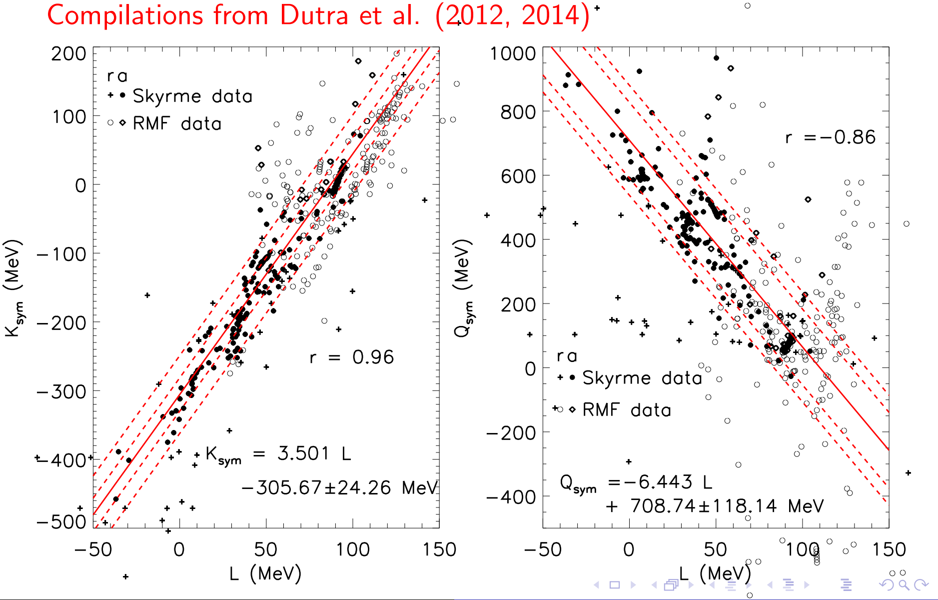

More Realistic Exclusion Region

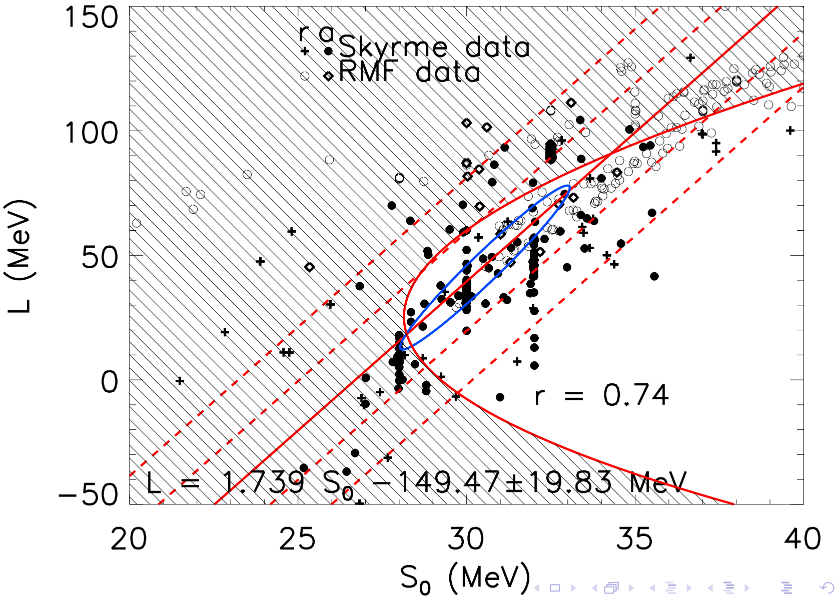

Analytic Approximation for the Boundary

$$S(u_t) = S^{\rm LB}(u_t), \qquad \left(\frac{dS}{du}\right)_{u_t} = \left(\frac{dS^{\rm LB}}{du}\right)_{u_t}$$

gives

$$S_0 + \frac{L}{3}(u_t - 1) + \frac{K_{sym}}{18}(u_t - 1)^2 = E_{\rm UG,0} u_t^{2/3} + B - \frac{K_s}{18}(u_t - 1)^2$$

$$L + \frac{K_{sym}}{3}(u_t - 1) = 2E_{\rm UG,0} u_t^{-1/3} - \frac{K_s}{3}(u_t - 1)$$

Assume $K_n = 3L$ (i.e., $K_{\rm sym} \approx 3L - K_s$). Then

$$S_0 = \frac{E_{\rm UG,0}}{3u_t^{4/3}}(1 + 2u_t^2) - E_0, \qquad L = \frac{2E_{\rm UG,0}}{u_t^{4/3}}$$

or after eliminating u_t,

$$S_0 = \frac{L}{6}\left[1 + 2\left(\frac{2E_{\rm UG,0}}{L}\right)^{3/2}\right] - E_0$$

Experimental Constraints

Isovector Skins and
Isobaric Analog States
from Danielewicz et al. (2017)

Other experimental constraints from Lattimer & Lim (2013)

Unitary gas constraints from
Tews et al. (2017)

Experimental and neutron matter constraints are compatible with unitary gas bounds.

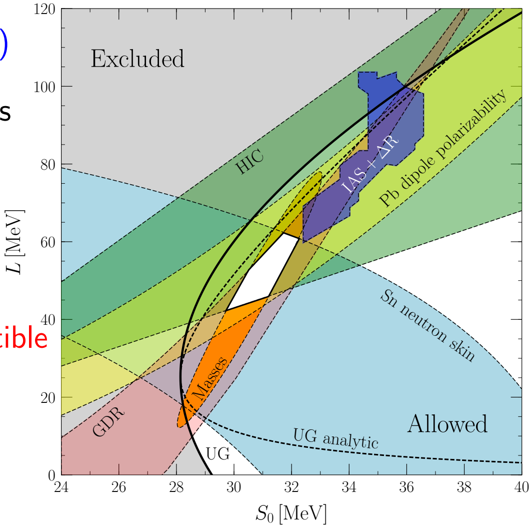

Piecewise Polytropes

Crust EOS is known: $n < n_0 = 0.4n_s$.

Read, Lackey, Owen & Friedman (2009) found high-density EOS can be modeled as piecewise polytropes with 3 segments.

They found universal break points ($n_1 \simeq 1.85n_s$, $n_2 \simeq 3.7n_s$) optimized fits to a wide family of modeled EOSs.

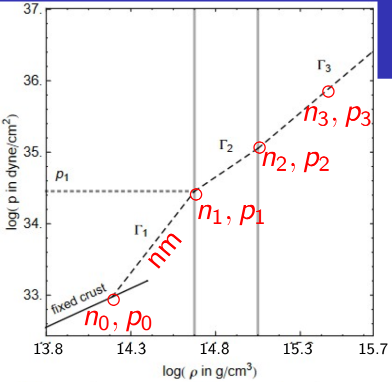

For $n_0 < n < n_1$, assume neutron matter EOS. Arbitrarily choose $n_3 = 7.4n_s$.

For a given p_1 (or Γ_1):
$0 < \Gamma_2 < \Gamma_{2c}$ or $p_1 < p_2 < p_{2c}$.
$0 < \Gamma_3 < \Gamma_{3c}$ or $p_2 < p_3 < p_{3c}$.

Minimum values of p_2, p_3 set by M_{max}; maximum values set by causality.

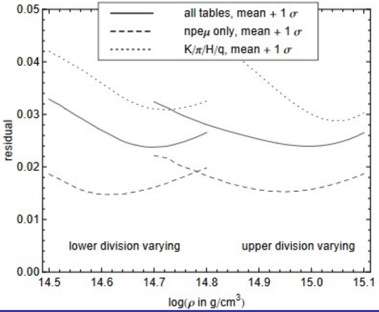

Maximum Mass and Causality Constraints

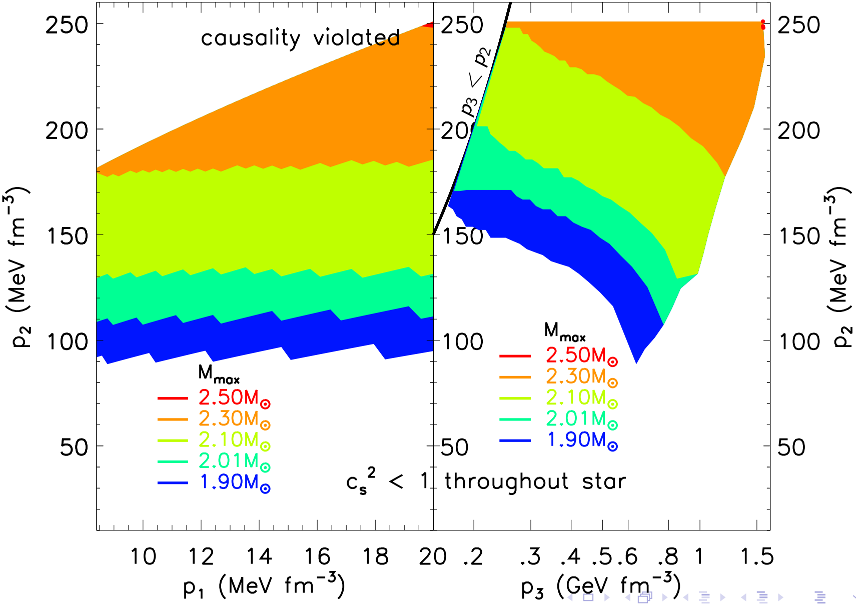

Mass-Radius Constraints from Causality

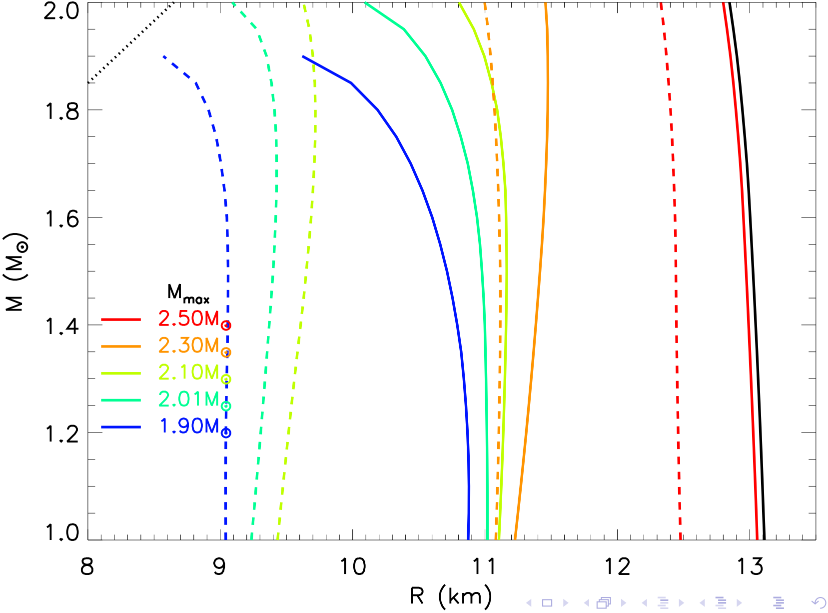

Photospheric Radius Expansion X-Ray Bursts

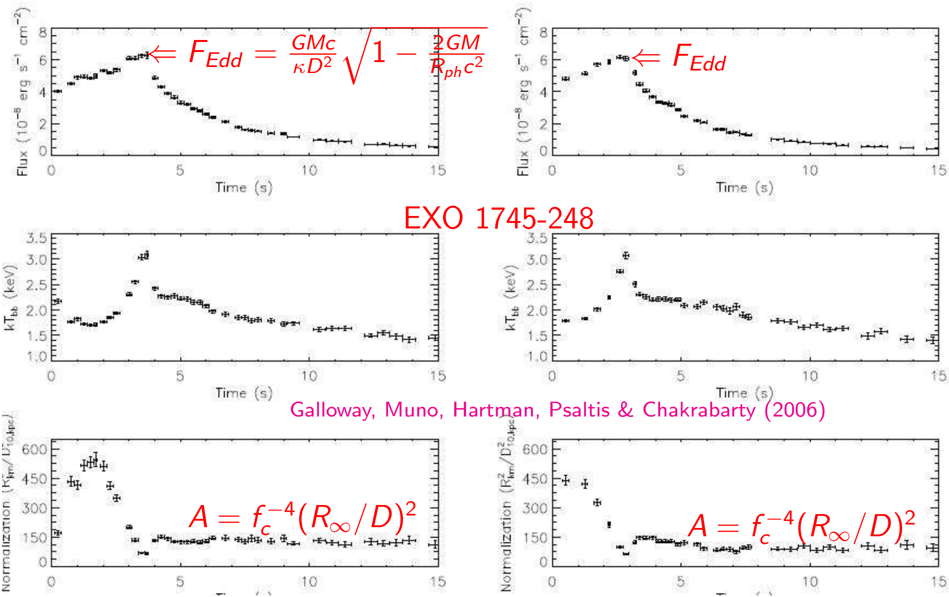

$\Leftarrow F_{Edd} = \frac{GMc}{\kappa D^2}\sqrt{1 - \frac{2GM}{R_{ph}c^2}}$

$\Leftarrow F_{Edd}$

EXO 1745-248

Galloway, Muno, Hartman, Psaltis & Chakrabarty (2006)

$A = f_c^{-4}(R_\infty/D)^2$

$A = f_c^{-4}(R_\infty/D)^2$

PRE Burst Model

Observations measure:

$$F_{Edd,\infty} = \frac{GMc}{\kappa D^2}\sqrt{1-2\beta}, \qquad \beta = \frac{GM}{Rc^2}$$

$$A = \frac{F_\infty}{\sigma T_\infty^4} = f_c^{-4}\left(\frac{R_\infty}{D}\right)^2$$

Determine parameters:

$$\alpha = \frac{F_{Edd,\infty}}{\sqrt{A}}\frac{\kappa D}{f_c^4 c^3} = \beta(1-2\beta)$$

$$\gamma = \frac{A f_c^4 c^3}{\kappa F_{Edd,\infty}} = \frac{R_\infty}{\alpha}.$$

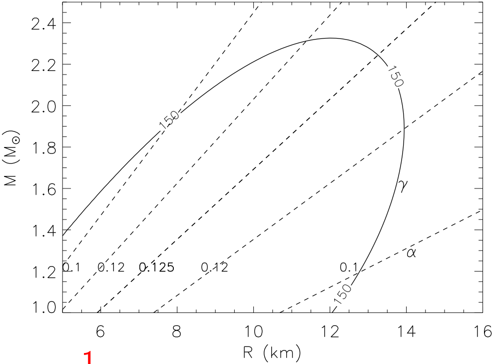

Solution:

$$\beta = \frac{1}{4} \pm \frac{\sqrt{1-8\alpha}}{4}, \qquad \alpha \le \frac{1}{8} \text{ for real solutions.}$$

PRE $M - R$ Estimates

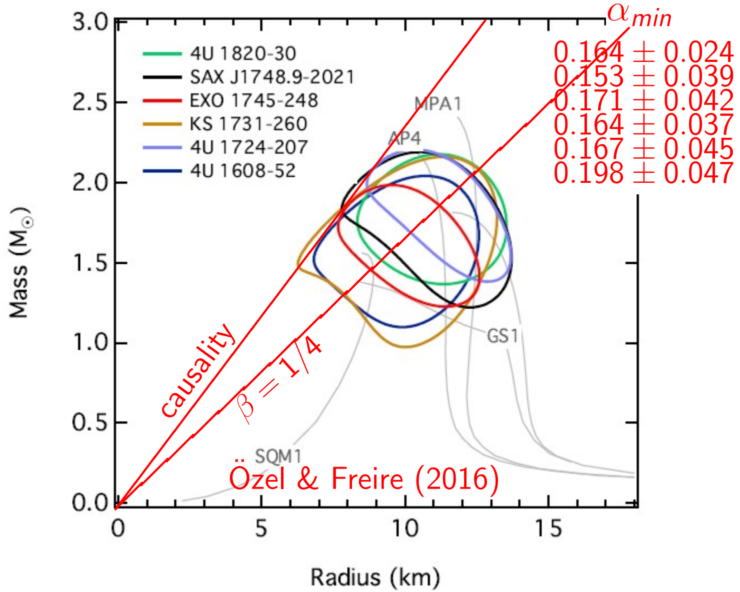

PRE Burst Models – Effect of Source Redshift

Ozel et al. $z_{\rm ph} = z$ $\quad \beta = GM/Rc^2 \quad$ Steiner et al. $z_{\rm ph} << z$

$$
\begin{aligned}
F_{\rm Edd} &= \frac{GMc}{\kappa D}\sqrt{1-2\beta} \\
A &= \frac{F_\infty}{\sigma T_\infty^4} = f_c^{-4}\left(\frac{R_\infty}{D}\right)^2 \\
\alpha &= \frac{F_{\rm Edd}}{\sqrt{A}}\frac{\kappa D}{F_c^2 c^3} = \beta(1-2\beta) \\
\gamma &= \frac{Af_c^4 c^3}{\kappa F_{\rm Edd}} = \frac{R_\infty}{\alpha} \\
\beta &= \frac{1}{4} \pm \frac{1}{4}\sqrt{1-8\alpha} \\
\alpha &\le \frac{1}{8} \text{ required.}
\end{aligned}
$$

$$
\begin{aligned}
F_{\rm Edd} &= \frac{GMc}{\kappa D} \\
\alpha &= \beta\sqrt{1-2\beta} \\
\theta &= \frac{1}{3}\cos^{-1}\left(1-54\alpha^2\right) \\
\beta &= \frac{1}{6}\left[1+\sqrt{3}\sin\theta - \cos\theta\right] \\
\alpha &\le \sqrt{\frac{1}{27}} \simeq 0.192 \text{ required.}
\end{aligned}
$$

QLMXB $M - R$ Estimates

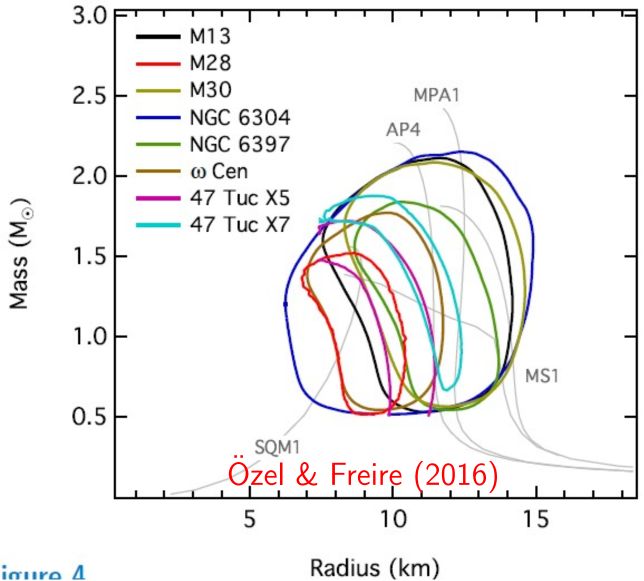

igure 4

Combined R fits

Assume $P(M)$ is that measured from pulsar timing ($\bar{M} = 1.4 M_\odot$).

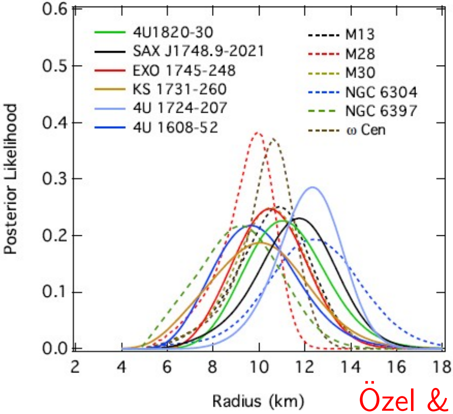

Özel & Freire (2015)

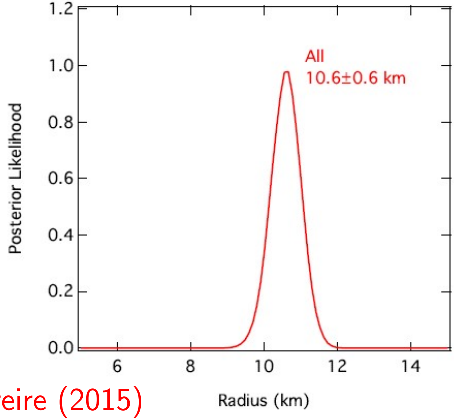

Role of Systematic Uncertainties

Systematic uncertainties plague radius measurements.

- Assuming uniform surface temperatures leads to underestimates in radii.
- Uncertainties in amounts of interstellar absorption
- Atmospheric composition: In quiescent sources, He or C atmospheres predict about 50% larger radii than H atmospheres.
- Non-spherical geometries: In bursting sources, the use of the spherically-symmetric Eddington flux formula leads to underestimate of radii.
- Disc shadowing: In bursting sources, leads to underprediction of $A = f_c^{-4}(R_\infty/D)^2$, overprediction of $\alpha \propto 1/\sqrt{A}$, and underprediction of $R_\infty \propto \sqrt{\alpha}$.

Piecewise-Polytrope Radius Distributions

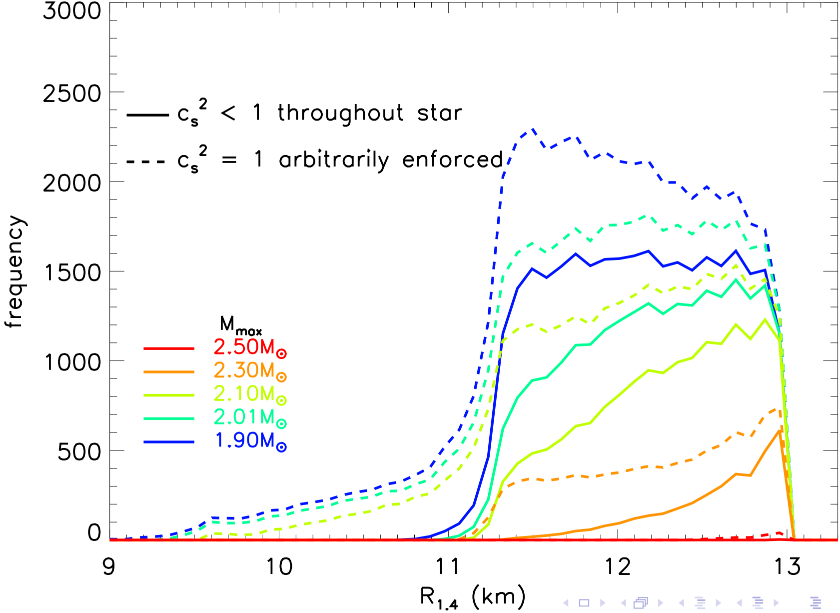

Folding Observations with Piecewise Polytropes

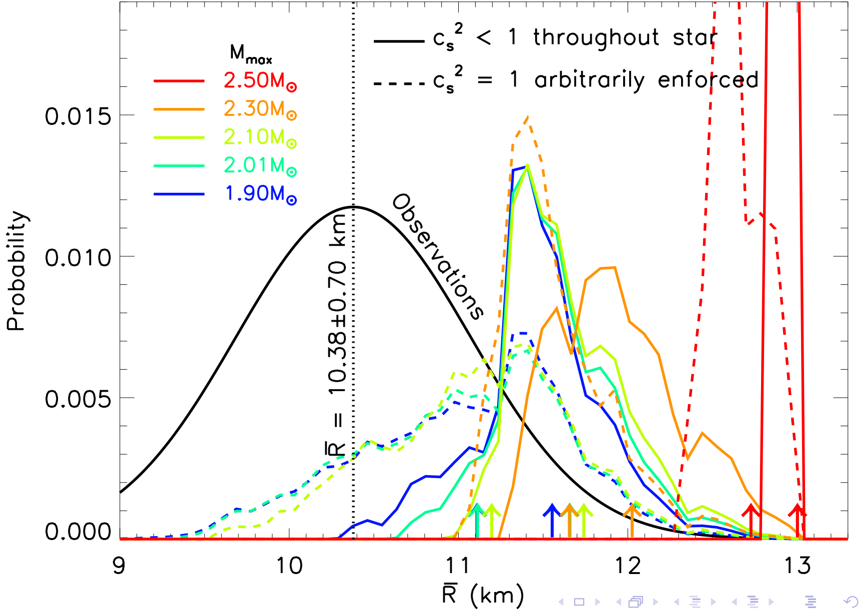

Other Studies

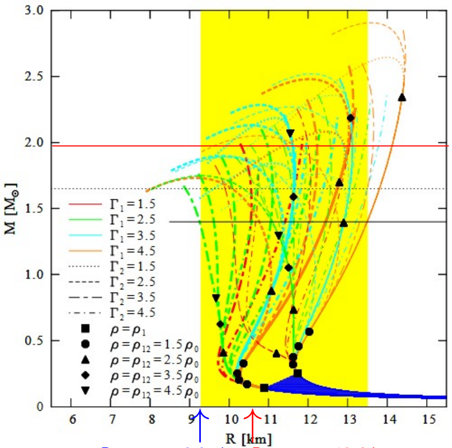

$R_{1.4,min} = 9.25$ km $R_{1.4,min} = 10.6$ km
$M_{max} = 1.66 M_\odot$ $M_{max} = 1.97 M_\odot$

Hebeler, Lattimer, Pethick & Schwenk 2010

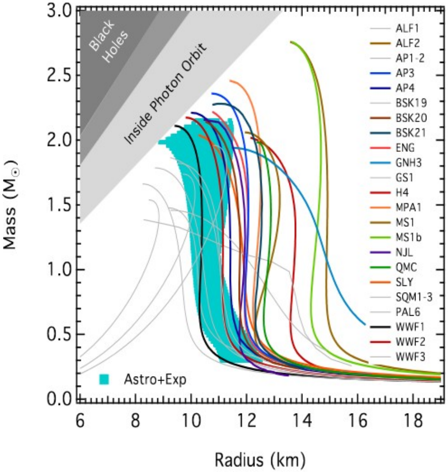

Özel & Freire 2016

Radius - p_1 Correlation

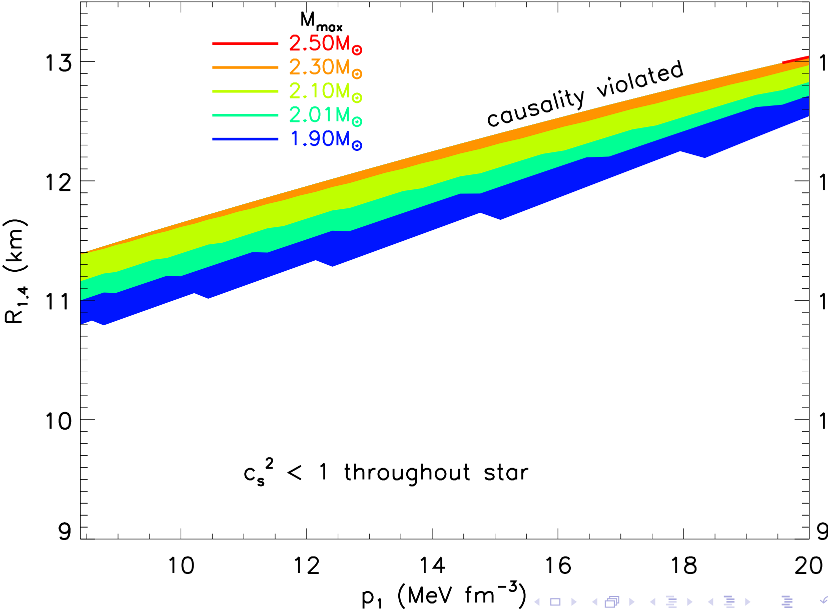

Binding Energy - Mass Correlations

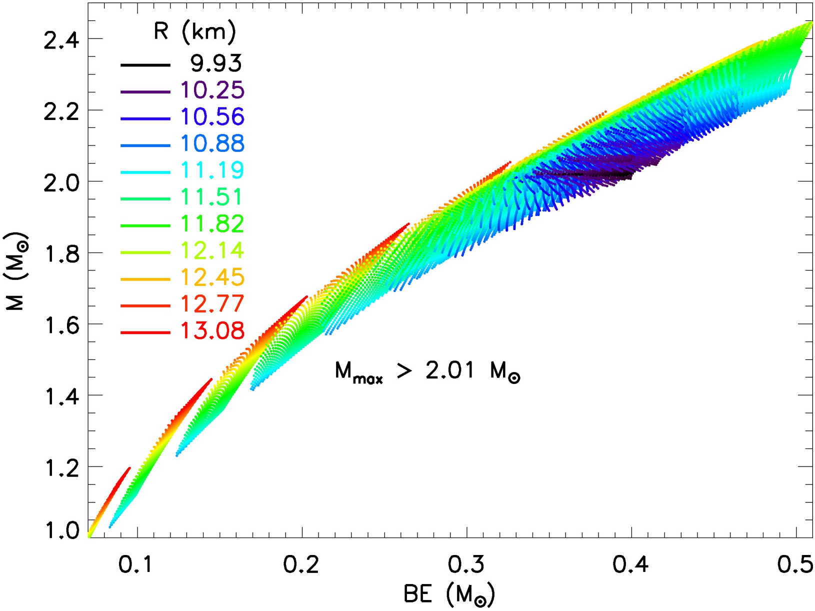

Binding Energy - Mass - Radius Correlations

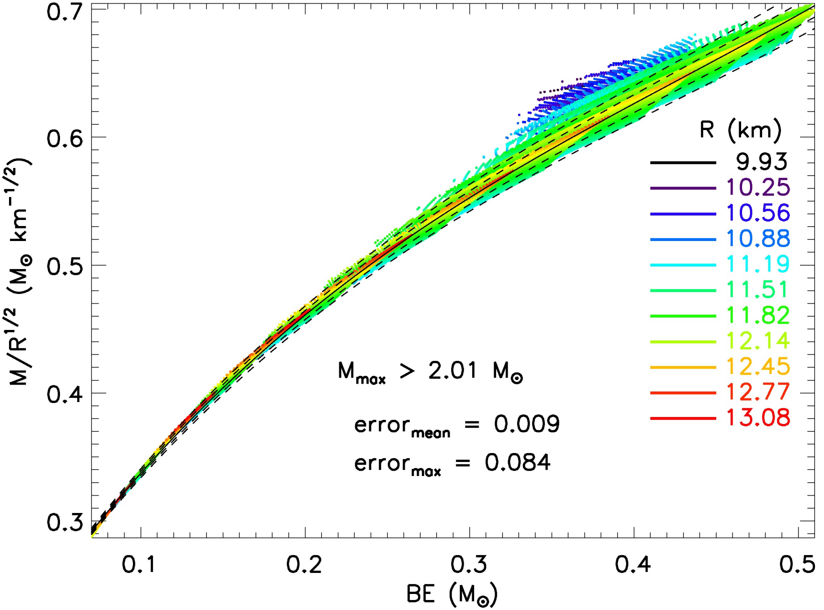

Moment of Inertia - Mass - Radius Correlations

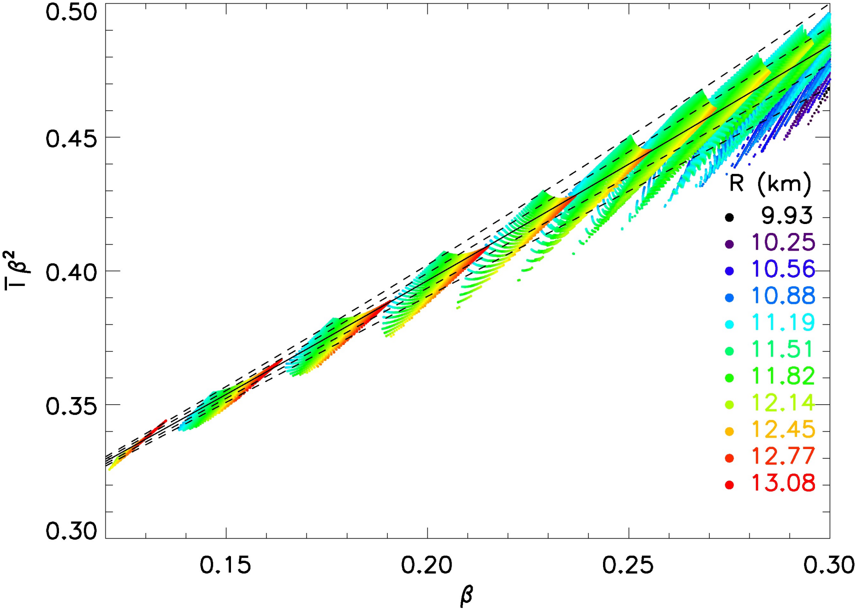

Moment of Inertia - Radius Constraints

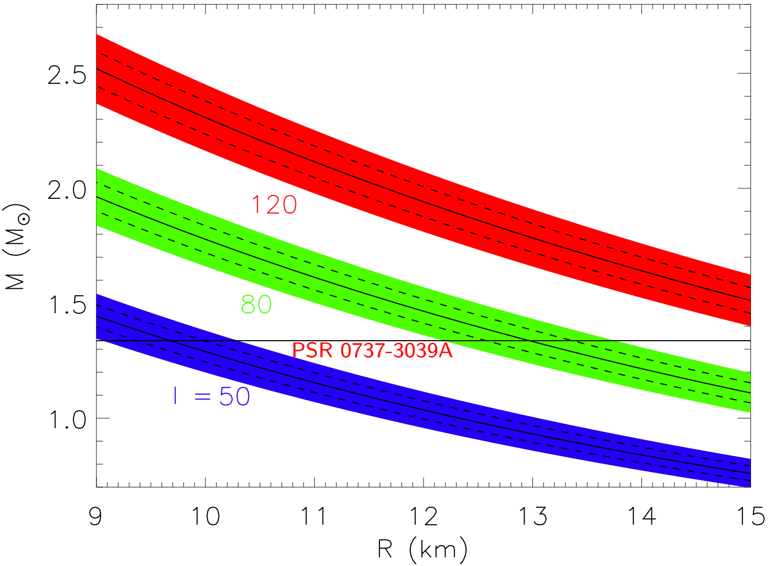

Tidal Deformatibility - Moment of Inertia

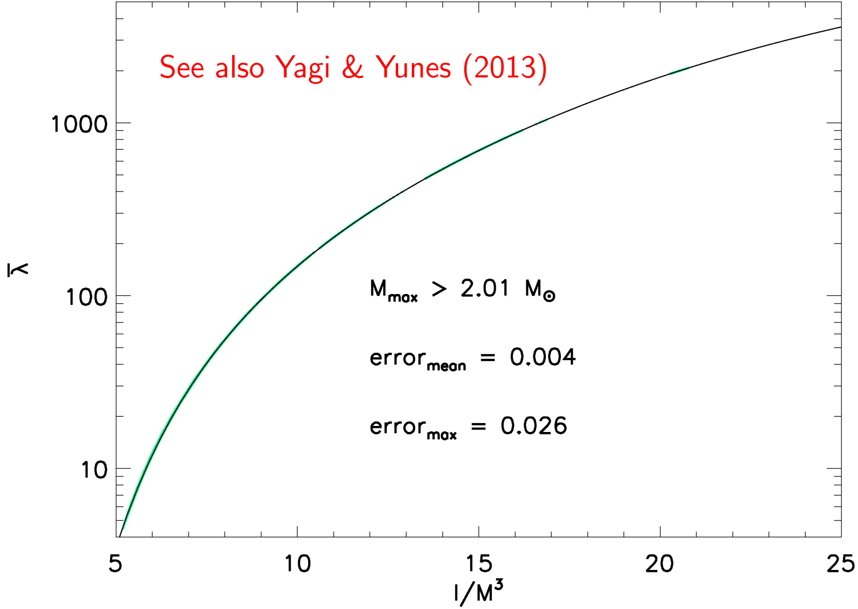

Tidal Deformatibility - Mass

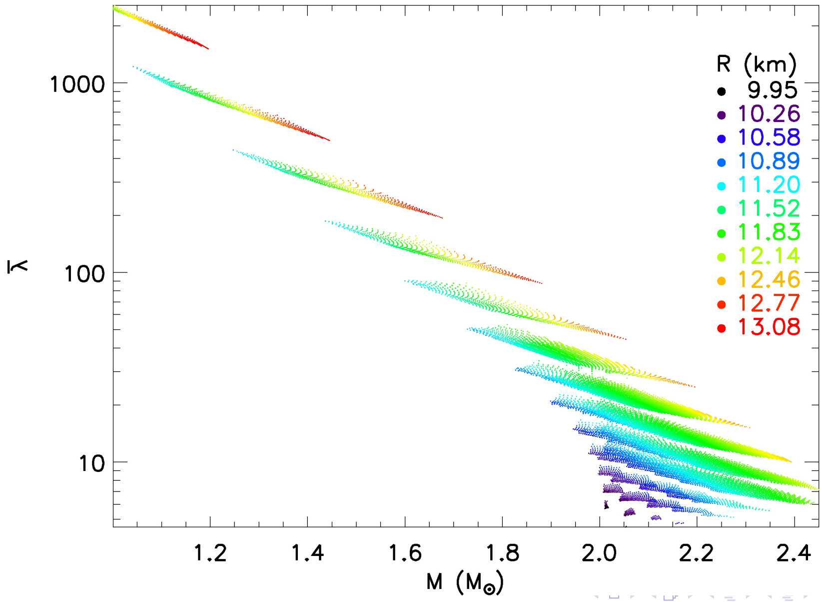

Tidal Deformability - Mass - Radius

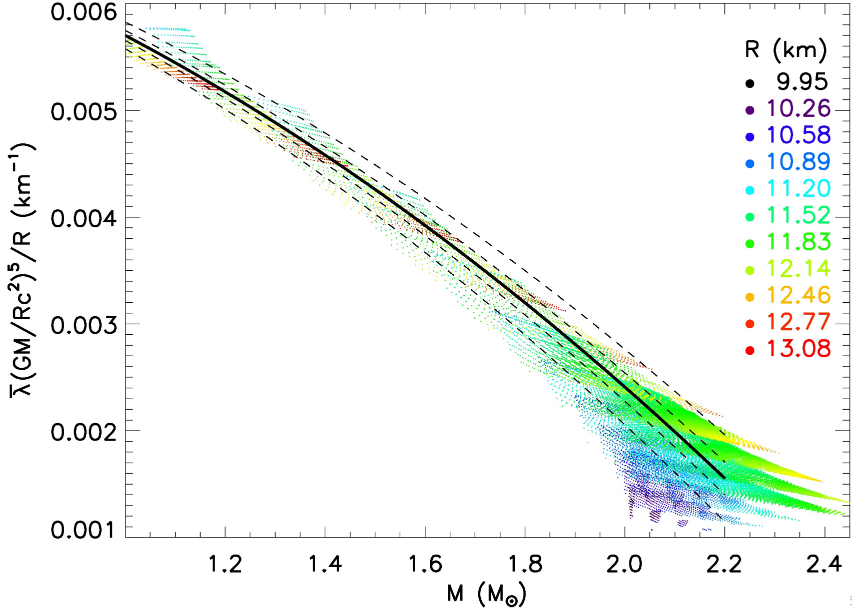

Binary Tidal Deformability

In a neutron star merger, both stars are tidally deformed. The most accurately measured deformability parameter is

$$\bar{\Lambda} = \frac{16}{13}\left[\bar{\lambda}_1 q^4(12q+1) + \bar{\lambda}_2(1+12q)\right]$$

where

$$q = \frac{M_1}{M_2} < 1$$

For $S/N \approx 20 - 30$, typical measurement accuracies are expected to be (Rodriguez et al. 2014; Wade et al. 2014):

$$\Delta M_{chirp} \sim 0.01 - 0.02\%, \qquad \Delta\bar{\Lambda} \sim 20 - 25\%$$

$$\Delta(M_1 + M_2) \sim 1 - 2\%, \qquad \Delta q \sim 10 - 15\%$$

Binary Tidal Deformatibility - $\bar{\Lambda}$

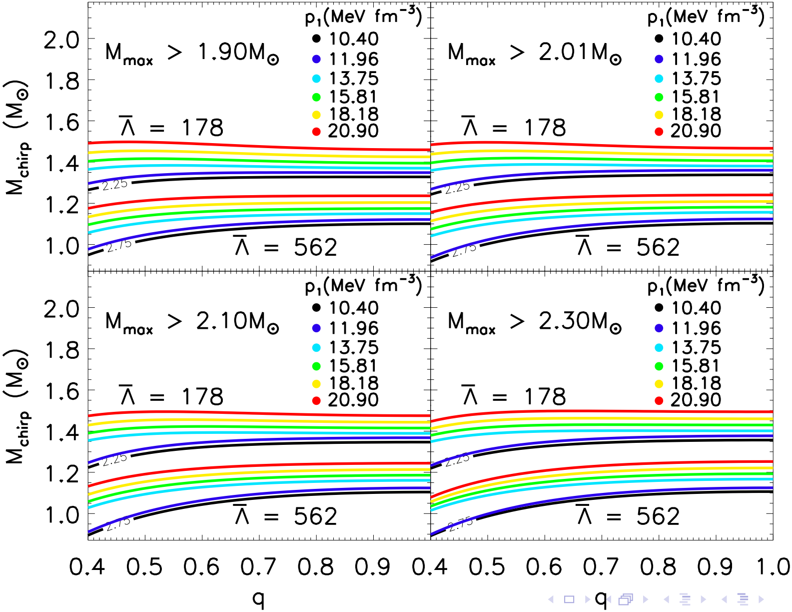

Binary Tidal Deformatibility - $M_{\rm chirp}$

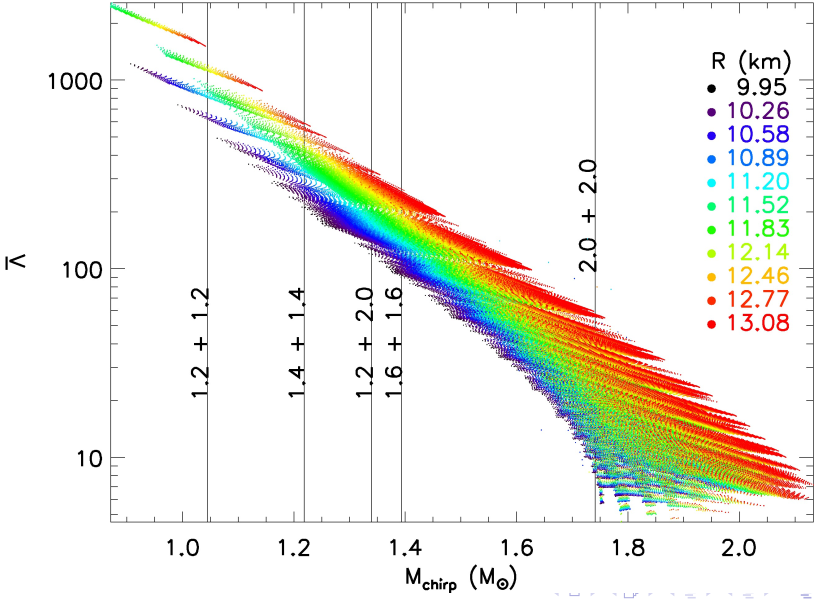

Binary Tidal Deformatibility - $M_{\rm chirp}$ - $R_{1.4}$

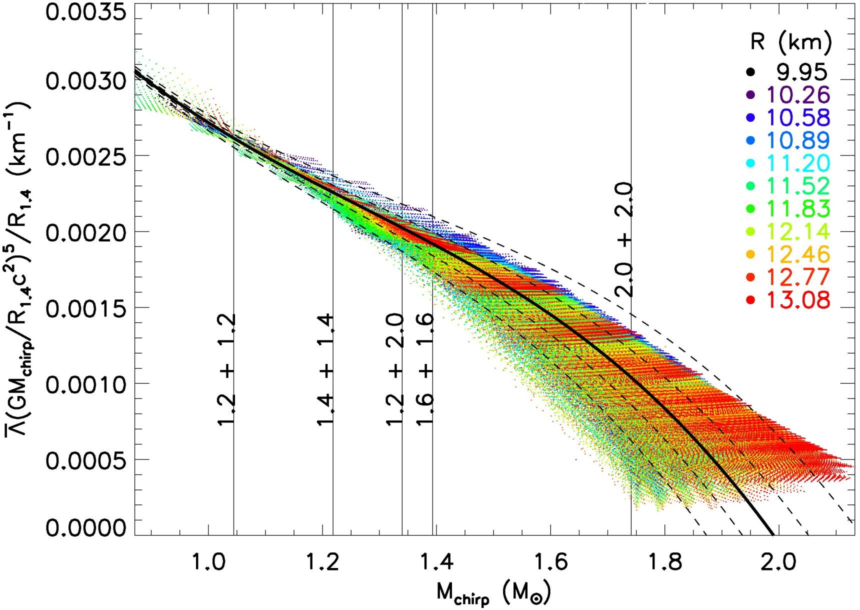

Hybrid Stars With First-Order Phase Transition

Tianqi Zhou

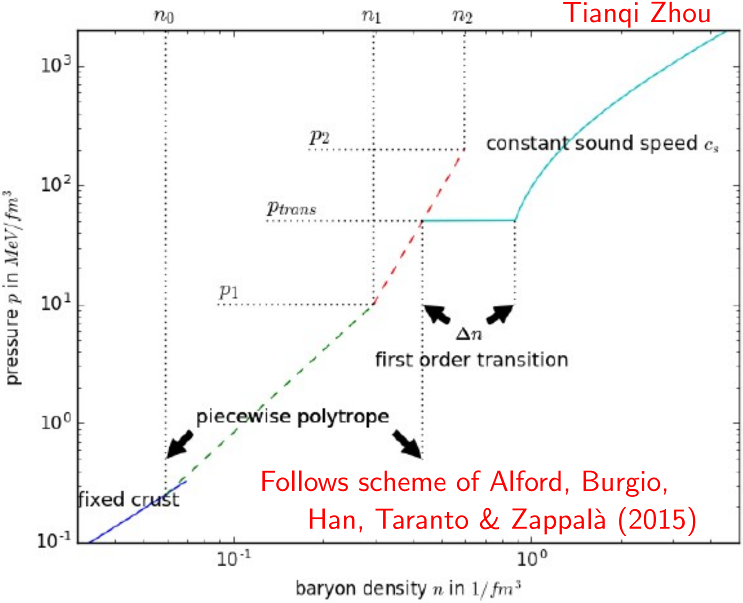

Follows scheme of Alford, Burgio, Han, Taranto & Zappalà (2015)

Mass-Radius Comparisons

Tianqi Zhou

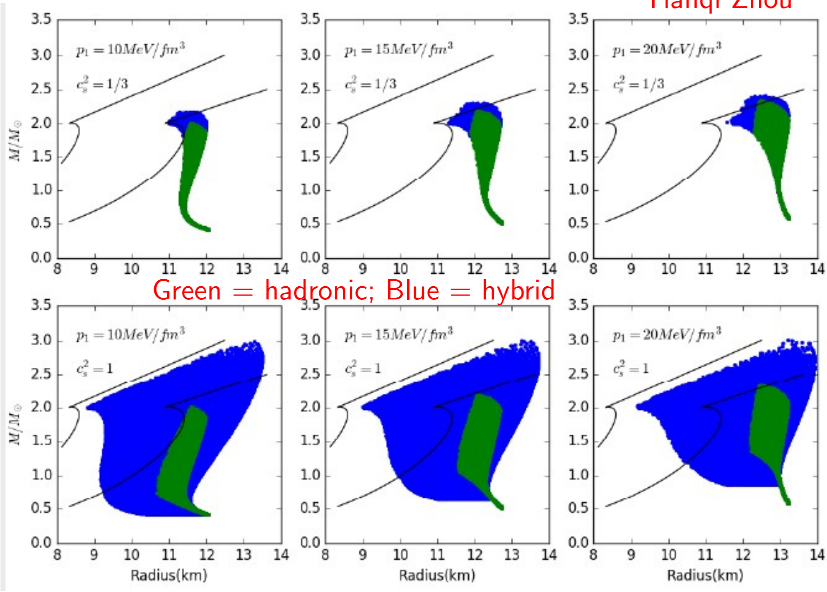

Green = hadronic; Blue = hybrid

Binding Energy - Compactness Comparisons

Tianqi Zhou

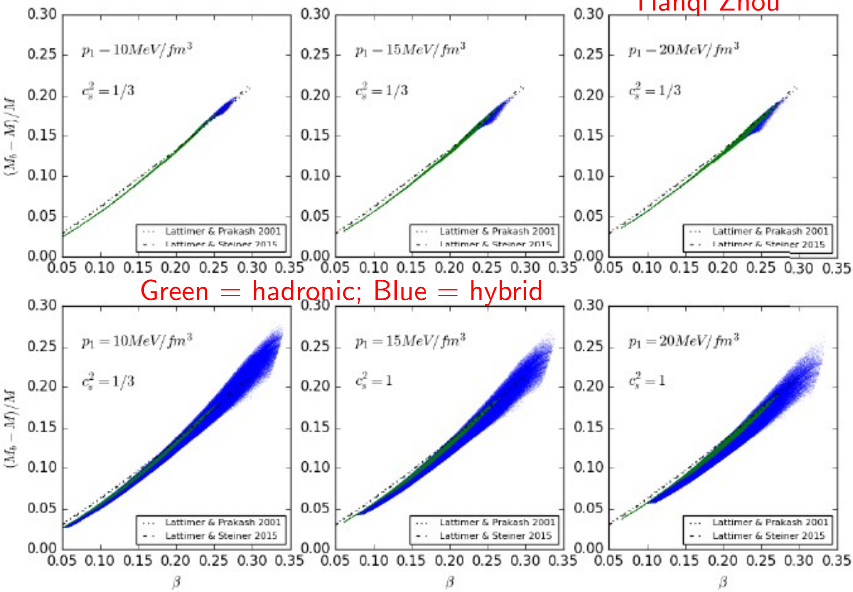

Green = hadronic; Blue = hybrid

Moment of Inertia - Compactness Comparisons

Tianqi Zhou

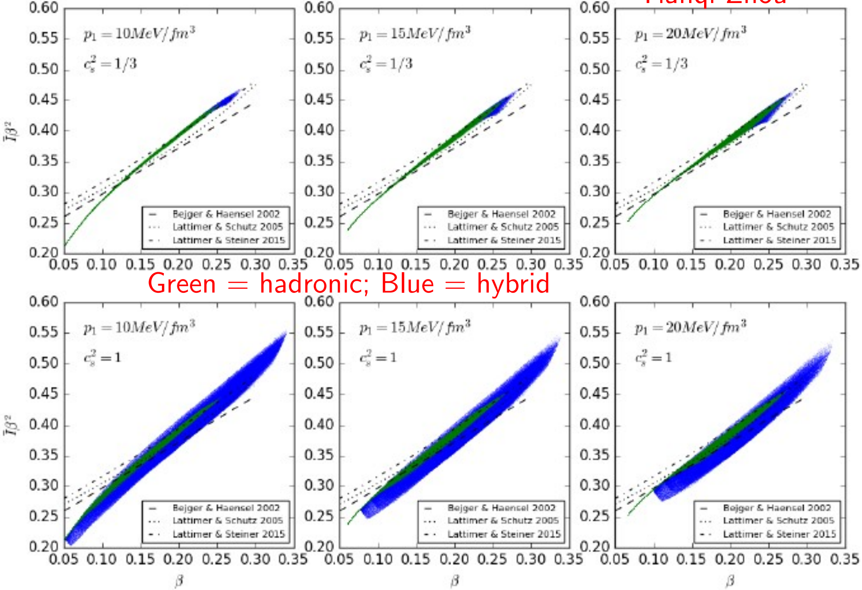

Green = hadronic; Blue = hybrid

Tidal Deformability Comparisons

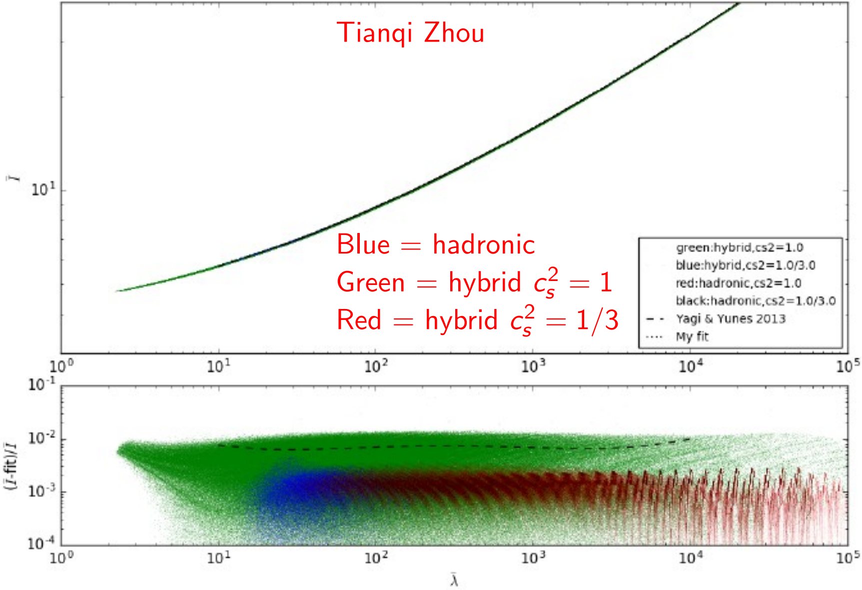

Future Observations

- Twin stars with different radii:
  Evidence for phase transitions
- Neutron star seismology and r-modes from GW observations:

$$\nu_{ellipticity} = 2f, \qquad \nu_{r-mode} \approx (4/3)f$$

  - Compactness from ν_{r-mode}.
  - Temperature if r-modes dominate heating.
  - Moment of inertia if r-modes dominate spindown.
  - Require factor of 3–10 improvement in sensitivity over aLIGO.
  - Potential sources would be very young.
- What else?

Additional Proposed Radius and Mass Constraints

- Pulse profiles Hot or cold regions on rotating neutron stars alter pulse shapes: NICER and LOFT will enable X-ray timing and spectroscopy of thermal and non-thermal emissions. Light curve modeling → M/R; phase-resolved spectroscopy → R.
- Moment of inertia Spin-orbit coupling of ultra- relativistic binary pulsars (e.g., PSR 0737+3039) vary i and contribute to $\dot{\omega}$: $I \propto MR^2$.
- Supernova neutrinos Millions of neutrinos detected from a Galactic supernova will measure BE$= m_B N - M$, $< E_\nu >$, τ_ν.
- QPOs from accreting sources ISCO and crustal oscillations

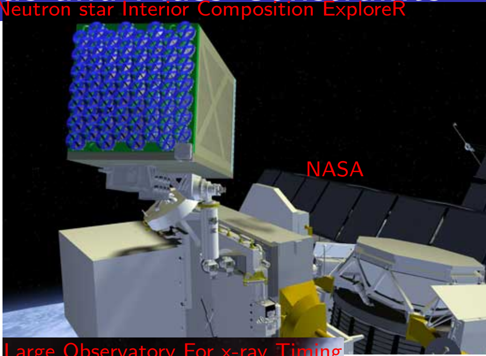

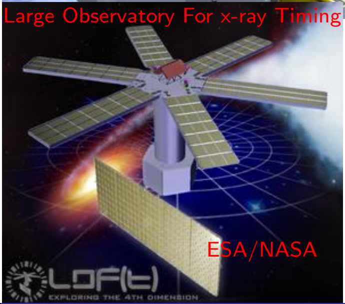

"Is Grandpa in the rocket ship?"

NICER successfully launched aboard a Falcon rocket, June 3.

Was powered up June 13.

Now taking data:

J0437-4715 ($1.44 M_\odot$)
J0030+0451
J1231-1411
J1614-2230 ($1.93 M_\odot$)

Science Measurements

NICER

Reveal stellar structure through lightcurve modeling, long-term timing, and pulsation searches

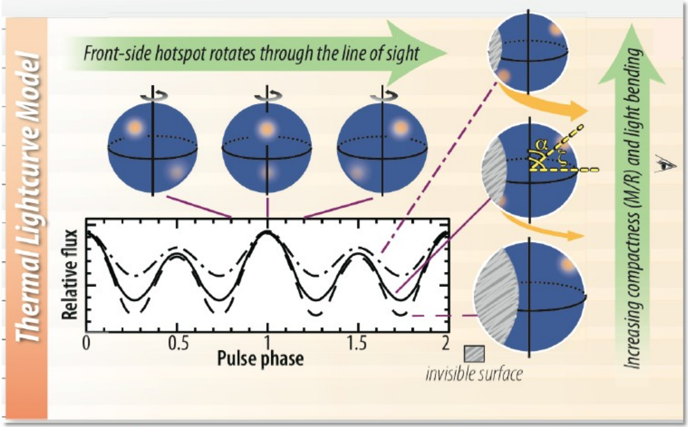

Lightcurve modeling constrains the compactness (*M*/*R*) and viewing geometry of a non-accreting millisecond pulsar through the depth of modulation and harmonic content of emission from rotating hot-spots, thanks to gravitational light-bending…

Science Measurements (cont.)

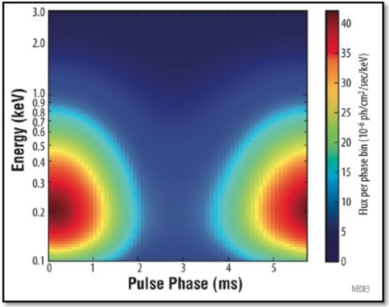

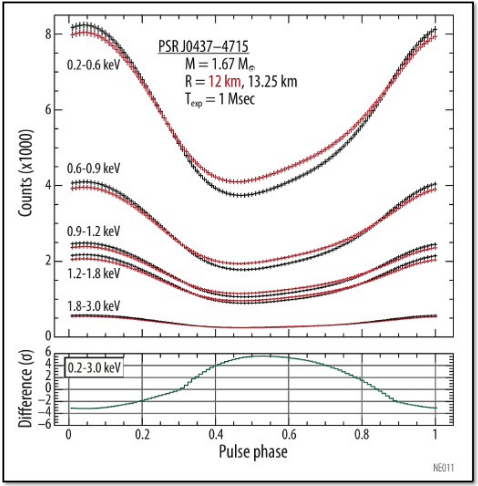

... while phase-resolved spectroscopy promises a direct constraint of radius *R*.

X-ray Timing of RXJ0720.4-3125

Hambaryan et al. (2017) undertook phase-resolved spectroscopy of the isolated neutron star RXJ0720.4-3125, one of "magnificent 7".

Spin period is 16.79s.

$T_{bb} \sim 90$ eV,

$T_{Fe} \sim 105$ eV.

$R_{1.4} \simeq 13.2 \pm 0.3$ km.